

# Bound States in the Continuum and Fano Resonances in the Dirac Cone Spectrum

Evgeny N. Bulgakov<sup>1,2</sup> and Dmitrii N. Maksimov<sup>1,2,3</sup>

<sup>1</sup>*Reshetnev Siberian State University of Science and Technology, 660037, Krasnoyarsk, Russia*

<sup>2</sup>*Kirensky Institute of Physics, Federal Research Center KSC SB RAS, 660036, Krasnoyarsk, Russia*

<sup>3</sup>*Siberian Federal University, Krasnoyarsk, 660041, Russia*

(Dated: May 13, 2019)

We consider light scattering by two dimensional arrays of high-index dielectric spheres arranged into the triangular lattice. It is demonstrated that in the case a triple degeneracy of resonant leaky modes in the Gamma-point the scattering spectra exhibit a complicated picture of Fano resonances with extremely narrow line-width. The Fano features are explained through coupled mode theory for a Dirac cone spectrum as a signature of optical bound states in the continuum (BIC). It is found that the standing wave in-Gamma BIC induces a ring of off-Gamma BICs due to different scaling laws for real and imaginary parts of the resonant eigenfrequencies in the Dirac cone spectrum. A quantitative theory of the spectra is proposed.

## I. INTRODUCTION

Photonic band engineering plays important role in modern science and technology<sup>1,2</sup>. Among numerous implementations the attention has been paid to photonic crystalline designs supporting Dirac cone spectrum about the  $\Gamma$ -point which pave a way to all-dielectric zero-refractive-index materials<sup>3,4</sup>. Recently zero-index all-dielectric metamaterials have been proposed<sup>5</sup> relying on the effect of optical bound states in the continuum (BICs) which are lossless localized solutions coexisting with the continuous spectrum of the scattering states<sup>6</sup>. The emergence of BICs is remarkable due to their effect on the scattering of electromagnetic waves. The BICs are known to induce sharp Fano<sup>7-11</sup> resonances in the scattering spectra due to interference between two optical pathways, the resonant pathway via the subradiant mode associated to the BIC and the direct pathways due to the non-resonant scattering<sup>11-15</sup>. In principle in the spectral vicinity of a BIC the Q-factor of the the resonances can be tuned to arbitrary high value once the material losses are neglected<sup>16,17</sup>. In this paper we examine the effect of the radiation losses on the spectrum of the leaky bands and Fano resonances about the Dirac point in a dielectric structure extended in two dimensions.

## II. SPECTRUM OF LEAKY MODES AND FANO RESONANCES

We consider a periodic two-dimensional array of high-contrast ( $\epsilon = 15$ ) dielectric spheres of radius  $R$  arranged into a triangular lattice in  $x0y$ -plane with period  $a$  as shown in Fig. 1. Further on the frequency will be expressed in terms of the vacuum wavevector  $k_0$ . To recover the optical properties of the system we employ The Korringa-Kohn-Rostoker method that was adapted to scattering of EM waves by 2D arrays of dielectric spheres by Ohtaka<sup>18,19</sup>. The method was later generalized for finding the band structure<sup>20</sup>.

The triangular lattice complies with  $C_{6v}$  point symmetry group<sup>21</sup> which has four one-dimensional

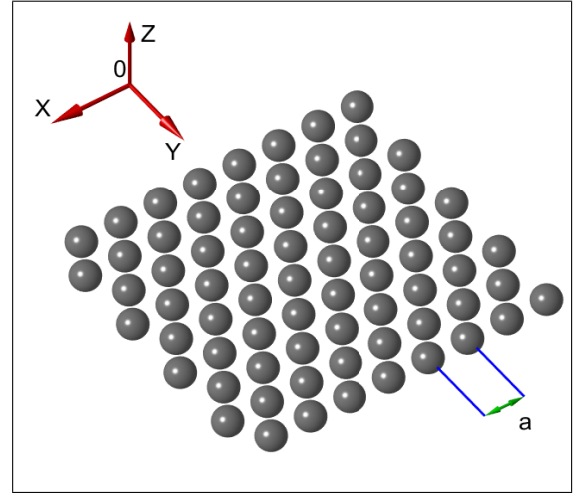


FIG. 1. Triangular lattice of dielectric spheres.

( $A_1, A_2, B_1, B_2$ ) and two two-dimensional representations ( $E_1, E_2$ ). According to Sakoda<sup>22</sup> a Dirac cone can be engineered through a triple degeneracy between two modes,  $p_x$  and  $p_y$ , of irreducible representation  $E_1$ , and one mode,  $s$ , of irreducible representation  $A_1$  in the  $\Gamma$ -point.  $p_x$  and  $p_y$  have the same frequency  $\Omega_1$  in the  $\Gamma$ -point, since they are of the same irreducible representation. The  $s$  mode, though, generally has a different frequency  $\Omega_2$ . The degeneracy  $\Omega_1 = \Omega_2$  is accidental in nature and be obtained by tuning the radius of the spheres. In case  $\epsilon = 15$  the degeneracy is found at  $R = 0.4705a$ . Once the degeneracy is achieved the spectrum in the vicinity of the  $\Gamma$ -point consists of an isotropic Dirac cone and a quadratic dispersion surface<sup>22</sup>.

The spectrum of the leaky modes against the  $x$ -component of the wavevector,  $k_x$  is shown in Fig. 2. One can see in Fig. 2 that the real parts of the eigenfrequencies demonstrate a behavior very close to that predicted in<sup>22</sup> with two bands forming a Dirac cone while the third, weakly dispersive band is parabolic. The Dirac spectrum in  $x0z$  plane is formed by hybridization between  $s$ - and  $p_x$ -modes which both have their electric fields antisym-

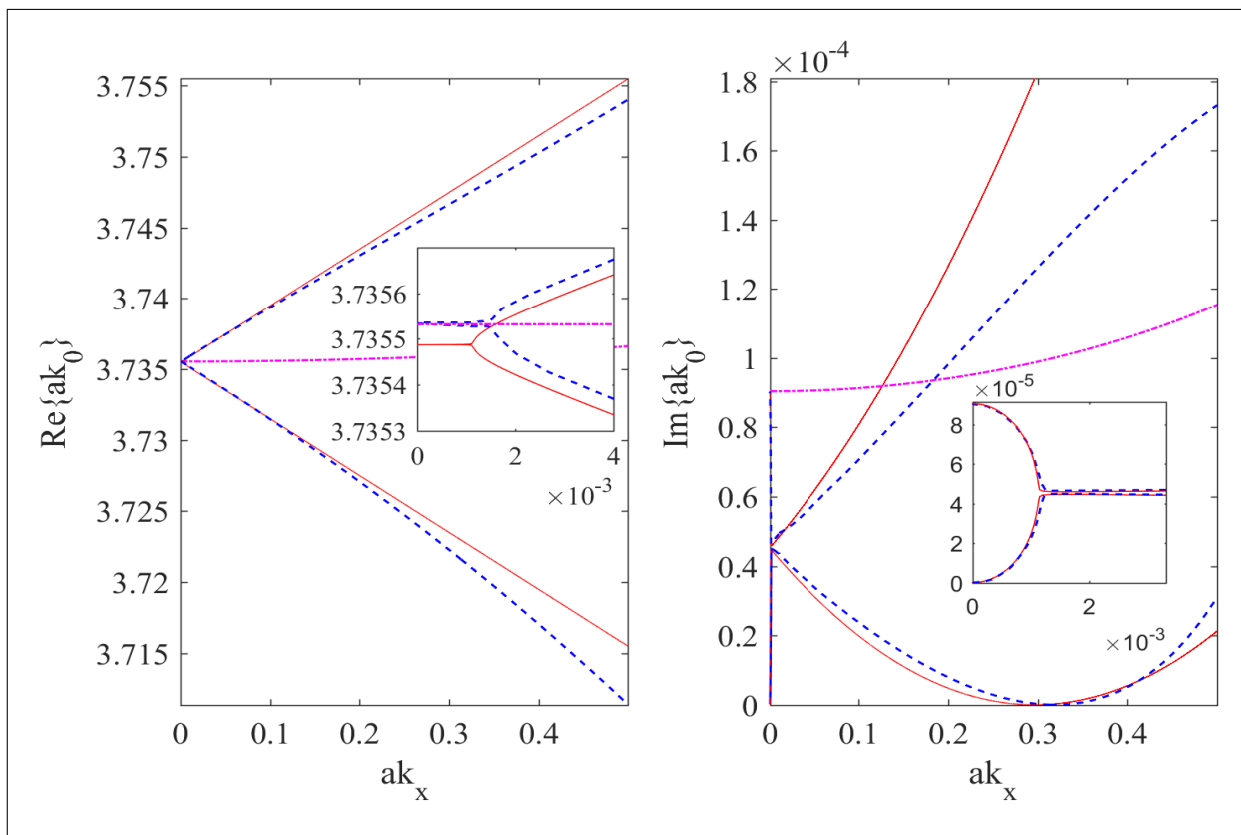


FIG. 2. The spectrum of leaky bands in the vicinity of the  $\Gamma$ -point. The real part of the eigenfrequency - left panel, the imaginary part - right panel. The insets resolve the spectra to  $ak_x \approx 10^{-3}$ . The dash blue lines show the spectrum of the hybridized modes, dash-dot magenta -  $p_y$ -mode. The red lines are eigenvalues of the matrix Eq. (3).

metric with respect to  $y \rightarrow -y$ . Notice that the radiation losses result in an anomaly in the spectrum with the dispersion deviating from a Dirac cone at small values of  $k_x$  as it is seen from the insets. That anomaly associated with an exceptional point has been considered in detail by Zhen and co-authors<sup>23</sup>.

More interesting, though, is the behavior of the imaginary parts of the eigenfrequency which correspond to the widths of the resonances. In the  $\Gamma$ -point the low frequency band obtains zero imaginary parts which indicates the emergence of symmetry protected BIC - standing wave decoupled from outgoing waves by symmetry<sup>5</sup>. The other two modes,  $p_x$  and  $p_y$  are leaky in the  $\Gamma$ -point. With a slightest off-set in the  $k$ -space the imaginary parts undergo dramatic changes due to hybridization between  $s$ - and  $p_x$ -modes. That results in almost equal imaginary parts at  $ak_x \approx 10^{-3}$ . Then the imaginary part of the high frequency band gradually increased with  $k_x$ , while the imaginary part of the low frequency band drops to zero at  $ak_x \approx 0.317$  where we find the second BIC. Since the BICs of that type have non-zero wave vector along the axis of periodicity of the structure, they are termed Bloch BICs<sup>12</sup>.

Next we propose a simple phenomenological approach explaining the structure of the spectrum in Fig. 2. Ac-

cording to<sup>22</sup> the spectrum of hybridized modes of  $E_1$  and  $A_1$  representations is found as the eigenvalues of the "Hamiltonian" matrix

$$C_0 = \begin{pmatrix} 0 & 0 & bk_x \\ 0 & 0 & bk_y \\ b^*k_x & b^*k_y & 0 \end{pmatrix}, \quad (1)$$

where  $b$  is a constant which can be evaluated by solving Maxwell's equations numerically<sup>22</sup>. Assume that the propagation direction of the incident wave is orthogonal to the  $y$ -axis, i.e.  $k_y = 0$ . Then Eq. (1) is reduced to  $2 \times 2$  matrix

$$H_0 = \begin{pmatrix} 0 & bk_x \\ b^*k_x & 0 \end{pmatrix}, \quad (2)$$

The radiation losses can be incorporated to Eq. (2) by applying coupled mode theory<sup>24</sup> for the hybridized resonances in the following manner

$$H = H_0 + \frac{i}{2}W^\dagger W, \quad (3)$$

where  $W^\dagger = (\sqrt{\gamma_p}, \sqrt{\gamma_s})$  with  $\gamma_s$  and  $\gamma_p$  being the decay rates of the hybridizing  $s$ - and  $p_x$ -modes into the  $TE$ -wave radiation channel with  $TE$ -outgoing (incoming) wave being defined as that whose electric vector is

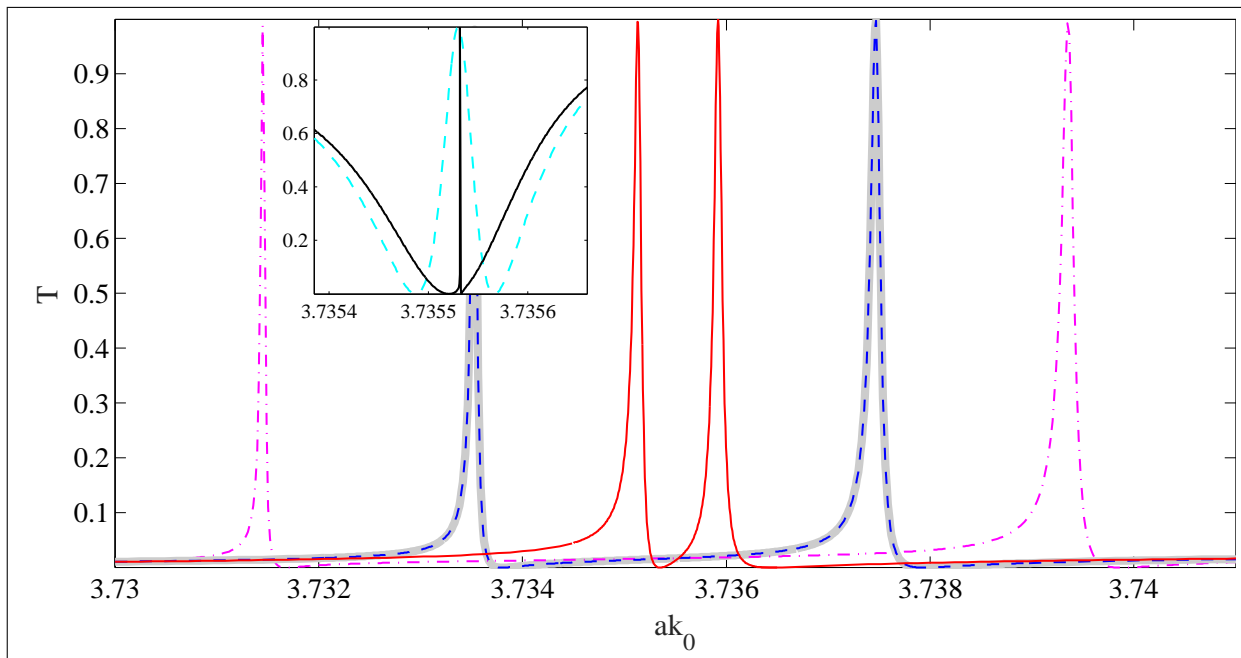


FIG. 3. Transmittance spectrum of the  $TE$ -wave,  $k_y = 0$ . Red line -  $ak_x = 0.01$ , blue dash line -  $ak_x = 0.05$ , dash-dot magenta -  $ak_x = 0.1$ . The inset shows the resonant feature in the vicinity of the exceptional point, teal dash line -  $ak_x = 10^{-3}$ , solid black -  $ak_x = 8 \cdot 10^{-5}$ . The thick gray line shown the case of the  $TE$ -wave with  $ak_x = 0, ak_y = 0.05$ .

perpendicular to the plane of incidence. Notice that for  $k_y = 0$  the hybridized modes are decoupled from the  $TM$ -wave by symmetry. Having in mind the definition Eq. (3), the quantity  $\gamma_p$  can be found from Fig. 2 as one half of the imaginary part of the resonant eigenfrequency of the  $p_x$ -mode in the  $\Gamma$ -point. On the other hand,  $\gamma_s$  in the vicinity of the  $\Gamma$ -point must be a dispersive quantity to reflect the singular nature of the symmetry protected BIC<sup>13</sup>. The leading term in the  $k_x$  expansion of  $\gamma_s$  is quadratic since  $k_x = 0$  is absolute minimum of the line width corresponding to the symmetry protected BICs. The dispersion of  $\gamma_s$  can be accessed by slightly detuning the radius  $R$  to lift the degeneracy so the individual features of the  $s$ -mode can be resolved. By running simulations with  $R = 0.4514$  one finds  $a\gamma_s = 1.028 \cdot 10^{-3} \cdot k_x^2$ . Finally, the parameter  $b$  can be found via perturbative approach in<sup>22</sup> or simply extracted from Fig. 2 as the real parts repulsion rate away off the feature at  $ak_x \approx 10^{-3}$ . Here we found  $b = 0.04$ . In Fig. 2 we demonstrate the spectrum of the matrix Eq. (3) that is found to be in quantitative agreement with numerical data. One can see that the model predicts the emergence of the satellite Bloch BIC as well as the anomalous spectral feature in the immediate vicinity of the  $\Gamma$ -point.

Now, let us discuss the effect of the spectra on the scattering. It is known that the presence of high-Q leaky modes results in narrow Fano feature which collapse as the spectral parameters are tuned to a BIC<sup>11–13,15</sup>. In our situation away off the exceptional point the  $TE$ -wave scattering should reveal two isolated Fano resonances whose positions are given by the real parts of the Dirac

cone eigenfrequencies while the width is controlled by the imaginary part of the spectrum. That statement is in full agreement with the numerical data shown in Fig. (3). In the vicinity of the exceptional point the Fano resonances merge into a single feature which can be only resolved on zoomed scale in  $k_0$  as shown in the inset in Fig. (3). Finally, we mention in passing that  $TM$ -waves are only coupled to the single parabolic band resulting to a single, almost non-dispersive Fano feature.

### III. RING OF BICS

What is remarkable according to Eq. (1) the Dirac cone is isotropic in the momentum space in the vicinity of the  $\Gamma$ -point. Let us see whether the presence of the radiation losses breaks that symmetry. Let specify the propagation direction specified by arbitrarily azimuthal angle  $\phi$  such that  $k_x = k_{\parallel} \cos(\phi)$  and  $k_y = k_{\parallel} \sin(\phi)$  with  $k_{\parallel} = \sqrt{k_x^2 + k_y^2}$ . The Hamiltonian has to be written in the following form<sup>24</sup>

$$C = C_0 + \frac{i}{2} W^\dagger W \quad (4)$$

where  $W$  is a  $2 \times 3$  matrix composed of the row matrices,  $W = [W_{TE}, W_{TM}]$ , that describe the coupling with  $TE$  and  $TM$ -waves, correspondingly. Taking into account that  $p_x \rightarrow p_y$  and  $p_y \rightarrow -p_x$  under rotation by  $\phi = \pi$  we can write

$$W_{TE} = [\sqrt{\gamma_p} \cos(\phi), \sqrt{\gamma_p} \sin(\phi), \sqrt{\gamma_s}], \quad (5)$$

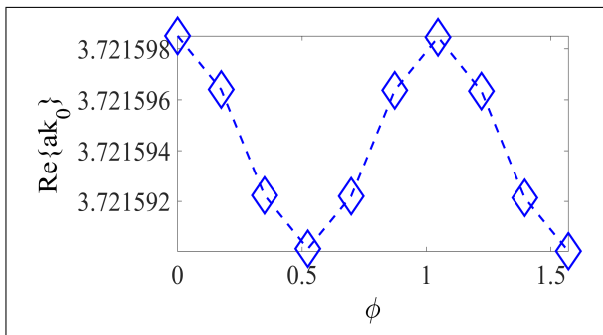


FIG. 4. Eigenfrequencies of the off- $\Gamma$  BICs as the function of the azimuthal angle  $\phi$ .

$$W_{TM} = [-\sqrt{\gamma_p} \sin(\phi), \sqrt{\gamma_p} \cos(\phi), 0]. \quad (6)$$

Next, one can easily check that after transforming the Hamiltonian  $C' = R^\dagger C R$  with matrix  $R$

$$R = \begin{pmatrix} \cos(\phi) & -\sin(\phi) & 0 \\ \sin(\phi) & \cos(\phi) & 0 \\ 0 & 0 & 1 \end{pmatrix}, \quad (7)$$

one finds

$$C' = \begin{pmatrix} 0 & 0 & bk_{\parallel} \\ 0 & 0 & 0 \\ b^*k_{\parallel} & 0 & 0 \end{pmatrix} + \frac{i}{2} \begin{pmatrix} \gamma_p & 0 & \sqrt{\gamma_s \gamma_p} \\ 0 & \gamma_p & 0 \\ \sqrt{\gamma_s \gamma_p} & 0 & \gamma_s \end{pmatrix}, \quad (8)$$

which reduces to Eq. (3) in terms of coupling to the  $TE$ -wave. Moreover, one can immediately see that the spectrum of complex eigenfrequencies is invariant under rotation. It means that our observation on the  $TE$ -wave scattering apply for any orientation of the plane of incidence given by  $\phi$ . This statement is illustrated in Fig. (3) for the incident wave with  $k_x = 0, ak_y = 0.05$ . Since the two-state model applies for any  $\phi$  the frequencies of the satellite Bloch BIC form a ring around the  $\Gamma$ -point.

In Fig. 4 we show the eigenfrequencies of the off- $\Gamma$  BICs as a function of the azimuthal angle  $\phi$ . One can see from Fig. 4 that the BICs form almost ideally circular ring with the lattice anisotropy footprint emerging only in the seventh significant digit. Let us consider the transmittance spectrum in the immediate vicinity of the off- $\Gamma$  BICs. Assume that the frequency of the incident wave is tuned to the lowest branch in Fig. 2. Then, if  $k_{\parallel}$  of the incident is matched to that of the leaky mode, the scattering spectrum of  $TE$ -waves exhibits an extremely narrow Fano feature whose profile is almost independent on the azimuthal angle. This is illustrated in Fig. 5 (upper panel) for  $ak_{\parallel} = 0.15$ . In the same subplot we also demonstrate that the resonant feature can be only observed with  $TE$ -waves while the transmittance of the  $TM$ -waves remains independent of frequency on the scale of the Fano resonance. Finally, on the further approach to the ring of BICs the lattice anisotropy emerges as a small shift of the resonance positions with respect to each other as seen from Fig. 5 (lower panel).

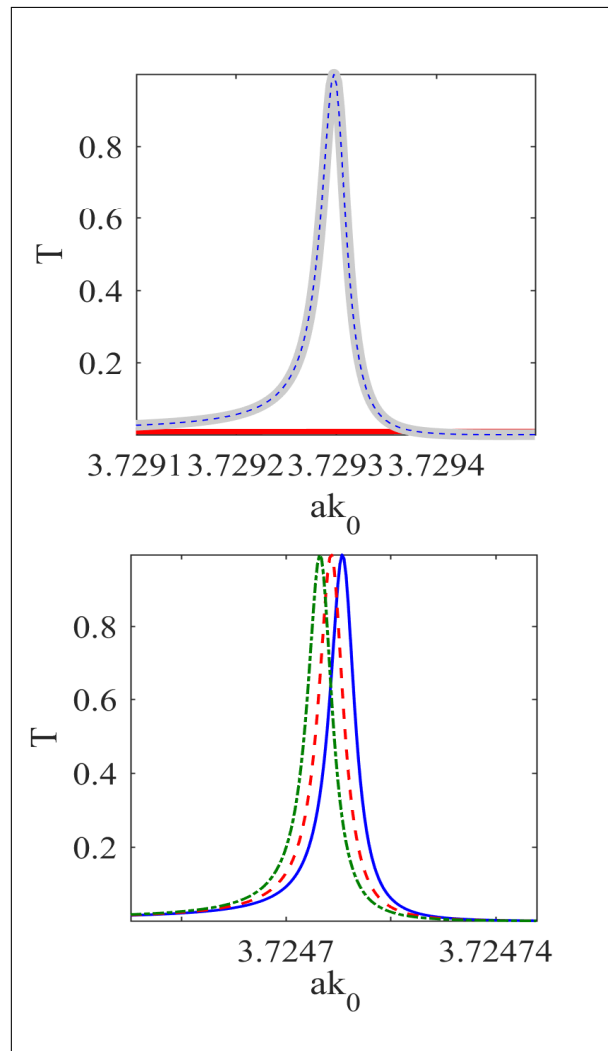


FIG. 5. Transmittance spectrum of  $TE$ -waves in the vicinity of the ring of BICs. Upper panel,  $ak_{\parallel} = 0.15$ ; thick gray line -  $\phi = 0$ , thin dash blue -  $\phi = \pi/2$ . Solid red line is the transmittance of  $TM$ -waves. Lower panel,  $ak_{\parallel} = 0.25$ ; solid blue -  $\phi = 0$ , dash red -  $\phi = \pi/4$ , dash-dot green -  $\phi = \pi/2$ .

#### IV. CONCLUSION

In summary, here we went beyond the ring of exceptional points predicted in<sup>23</sup> by taking into account the dispersion of the hybridized modes line widths. We have demonstrated that the presence of a Dirac cone in the  $\Gamma$ -point results in the emergence of high- $Q$  Fano resonances in the transmittance spectrum of  $TE$ -waves near the normal incidence. The positions and widths of the resonances can be estimated from a simple coupled mode approach leading to  $2 \times 2$  matrix whose parameters are easily extracted from the dispersion of the hybridized leaky modes. It is shown that in the vicinity of the  $\Gamma$ -point the scattering spectra are insensitive to the orientation of the plane of incidence. Most remarkably, it is found that the presence of a Dirac cone together with an in- $\Gamma$

symmetry protected BIC induces a ring of Bloch BICs surrounding the  $\Gamma$ -point the  $k$ -space. The emergence of the BICs in the model is a result of destructive interference between two resonant modes with the condition for BICs<sup>25</sup> being fulfilled by tuning the wavenumber due to the difference in asymptotic behavior between Hermitian and non-Hermitian parts of the matrix in Eq. (3). The presence of such BICs allows for fine tuning the width of Fano resonances by changing the angle of incidence. Recently, we have seen a big deal of interest to application

of Fano resonances to sensing and switching<sup>26–28</sup>. We believe that the proposed model may be a useful platform for engineering Fano resonances in all-dielectric set-ups<sup>29</sup>. The possibility of BICs eigenfrequencies forming a ring in momentum space has been recently pointed out in a view of multipolar decompositions<sup>30</sup>. We speculate that a further detailed analysis of multipolar structure could shed light onto interference mechanisms leading to BICs.

**Funding.** This work was supported by Ministry of Education and Science of Russian Federation (state contract N 3.1845.2017/4.6).

- 
- <sup>1</sup> Y. Ding and R. Magnusson, *Optics Express* **12**, 5661 (2004).
- <sup>2</sup> J. D. Joannopoulos, S. G. Johnson, J. N. Winn, and R. D. Meade, *Photonic crystals: molding the flow of light* (Princeton university press, 2011).
- <sup>3</sup> X. Huang, Y. Lai, Z. H. Hang, H. Zheng, and C. T. Chan, *Nature Materials* **10**, 582 (2011).
- <sup>4</sup> C. T. Chan, Z. H. Hang, and X. Huang, *Advances in OptoElectronics* **2012**, 1 (2012).
- <sup>5</sup> M. Minkov, I. A. D. Williamson, M. Xiao, and S. Fan, *Physical Review Letters* **121**, 263901 (2018).
- <sup>6</sup> C. W. Hsu, B. Zhen, A. D. Stone, J. D. Joannopoulos, and M. Soljačić, *Nature Reviews Materials* **1**, 16048 (2016).
- <sup>7</sup> J. Lee, B. Zhen, S.-L. Chua, W. Qiu, J. D. Joannopoulos, M. Soljačić, and O. Shapira, *Physical Review Letters* **109**, 067401 (2012).
- <sup>8</sup> C. S. Kim, A. M. Satanin, Y. S. Joe, and R. M. Cosby, *Physical Review B* **60**, 10962 (1999).
- <sup>9</sup> S. P. Shipman and S. Venakides, *Physical Review E* **71**, 026611 (2005).
- <sup>10</sup> A. F. Sadreev, E. N. Bulgakov, and I. Rotter, *Physical Review B* **73**, 235342 (2006).
- <sup>11</sup> C. Blanchard, J.-P. Hugonin, and C. Sauvan, *Physical Review B* **94**, 155303 (2016).
- <sup>12</sup> E. N. Bulgakov and A. F. Sadreev, *Physical Review A* **92**, 023816 (2015).
- <sup>13</sup> E. N. Bulgakov and D. N. Maksimov, *Journal of the Optical Society of America B* **35**, 2443 (2018).
- <sup>14</sup> E. Bochkova, S. Han, A. de Lustrac, R. Singh, S. N. Burokur, and A. Lupu, *Optics Letters* **43**, 3818 (2018).
- <sup>15</sup> A. A. Bogdanov, K. L. Koshelev, P. V. Kapitanova, M. V. Rybin, S. A. Gladyshev, Z. F. Sadrieva, K. B. Samusev, Y. S. Kivshar, and M. F. Limonov, *Advanced Photonics* **1**, 1 (2019).
- <sup>16</sup> L. Yuan and Y. Y. Lu, *Physical Review A* **95**, 023834 (2017).
- <sup>17</sup> E. Bulgakov and A. Sadreev, *Physical Review B* **98**, 085301 (2018).
- <sup>18</sup> K. Ohtaka, *Physical Review B* **19**, 5057 (1979).
- <sup>19</sup> K. Ohtaka, *Journal of Physics C: Solid State Physics* **13**, 667 (1980).
- <sup>20</sup> K. Ohtaka, Y. Suda, S. Nagano, T. Ueta, A. Imada, T. Koda, J. S. Bae, K. Mizuno, S. Yano, and Y. Segawa, *Physical Review B* **61**, 5267 (2000).
- <sup>21</sup> T. Inui, Y. Tanabe, and Y. Onodera, *Group theory and its applications in physics*, Vol. 78 (Springer Science & Business Media, 2012).
- <sup>22</sup> K. Sakoda, *Optics Express* **20**, 25181 (2012).
- <sup>23</sup> B. Zhen, C. W. Hsu, Y. Igarashi, L. Lu, I. Kaminer, A. Pick, S.-L. Chua, J. D. Joannopoulos, and M. Soljačić, *Nature* **525**, 354 (2015).
- <sup>24</sup> W. Suh, Z. Wang, and S. Fan, *IEEE Journal of Quantum Electronics* **40**, 1511 (2004).
- <sup>25</sup> A. Volya and V. Zelevinsky, *Physical Review C* **67**, 054322 (2003).
- <sup>26</sup> M. Heuck, P. T. Kristensen, Y. Elesin, and J. Mørk, *Optics Letters* **38**, 2466 (2013).
- <sup>27</sup> M. F. Limonov, M. V. Rybin, A. N. Poddubny, and Y. S. Kivshar, *Nature Photonics* **11**, 543 (2017).
- <sup>28</sup> Y. Zhang, W. Liu, Z. Li, Z. Li, H. Cheng, S. Chen, and J. Tian, *Optics Letters* **43**, 1842 (2018).
- <sup>29</sup> A. Krasnok, R. Savelev, D. Baranov, and P. Belov, in *World Scientific Handbook of Metamaterials and Plasmonics* (World Scientific, 2017) pp. 337–385.
- <sup>30</sup> Z. Sadrieva, K. Frizyuk, M. Petrov, Y. Kivshar, and A. Bogdanov, arXiv preprint arXiv:1903.00309 (2019).